ANALYSES OF THE DYNAMIC EFFECTS ON WINTER CIRCULATION OF THE TWO MAIN MOUNTAINS IN THE NORTHERN HEMISPHERE

I. RELATIONSHIP AMONG GENERAL CIRCULATION, TELECONNECTION AND STATIONARY WAVES

Zou Xiaolei (邹晓蕾), *Ye Duzheng* (叶笃正) and *Wu Guoxiong* (吴国雄)

Institute of the Atmospheric Physics, Academia Sinica, Beijing 100080

Received May 11, 1992

ABSTRACT

The distribution of troughs and ridges of geopotential height, the teleconnection patterns and the propagation patterns of stationary waves are the main features of the January mean geopotential height field at 500hPa. Data analyses and numerical experiments indicate that these three characteristics are associated to one another and closely related to the mechanical forcing of the Rocky Mountains and Tibetan Plateau. There exists a prominent negative correlation in the intensity variation between the American trough and the Asian trough at high and middle latitudes. Such negative correlation, in connection with the interannual variation of the intensity of the jets in front of the two troughs, leads to the existence of similar teleconnection patterns in North America and East Asia. On the other hand, the different propagation behaviour of quasi-stationary waves downstream of the two main mountains results in a fundamental difference in the distribution of correlation chains in North America and East Asia.

Key words: American trough, Asian trough, teleconnection patterns, effects of orography, stationary waves

I. INTRODUCTION

On monthly mean geopotential height field the westerlies in middle latitudes are superimposed by large-scale wave perturbations. From winter to summer, the north-south temperature difference and the east-west thermal difference between continents and oceans change tremendously. However, there is no corresponding change in the position of the American trough and the Asian trough at 500 hPa (Bolin, 1950). It seems that the latter might be related to the dynamic forcing of orography in middle latitudes. Since the pioneering work of Charney and Eliassen (1949), many researchers (for instance, Gambo, 1956; Murakami, 1963; Kasahara, 1966; Grose and Hoskins, 1976; etc.) indicated that the main mountain blocks—the Rocky Mountains and the Tibetan Plateau—play important roles in determining the trough and ridge system in the upper troposphere. Kasahara et al. (1973), Nigam (1983), and Jacqmin and Lindzen (1985) carried out a combined and separated simulation on the effects of orography, thermal forcing, and transient processes. They concluded that orography has an important effect on the formation of quasi-stationary planetary waves in the upper troposphere. Numerical simulations and data analyses of Blackman et al. (1977) and Lau (1978; 1979) showed further that the distribution and the structure of stationary waves have a major impact on the distribution of jets, the characteristics of transient waves, and the global or local general circulation.

Another important characteristic of the 500 hPa time mean field is that there exist different teleconnection patterns. For example, the five teleconnection patterns of Wallace and Gutzler (1981, referred to as WG hereafter). These teleconnection patterns are so evident that they are widely used both in scientific research and in operational applications.

The general circulation is a unique system and there must exist some relationship between the trough and ridge system and the different teleconnection patterns. Since the trough and ridge system as well as the teleconnection patterns are both the characteristics of the time mean field, they are not certainly uncorrelated. Although the two-dimensional Rossby wave dispersion theory (Hoskins et al., 1977; Hoskins and Karoly, 1981) has been used to explain the teleconnection problems, there are many teleconnection phenomena that can not be explained by wave propagation. The purpose of this paper is to understand the existing relationship between the trough and ridge system and teleconnection patterns by studying the dynamic effects of the Rocky Mountains and the Tibetan Plateau. The characteristic of the American trough and the Asian trough is analysed in Section II. The relationship between the variation of trough and ridge system and the teleconnection patterns in East Asia and North America is studied in Section III. The horizontal propagation of the orographic stationary waves in East Asia and North America is presented in Section IV. Conclusions are presented in Section V.

II. STRUCTURE AND VARIATION OF THE AMERICAN TROUGH AND THE ASIAN TROUGH

1. *Variations in Intensity and Position of the Two Main Troughs*

The variation of the 520 dgpm contour at 500 hPa of January mean geopotential height from 1951 to 1960 obtained from the NMC data shows that, when the intensity of the Asian trough decreases gradually from its maximum in 1956 to its minimum in 1957, the intensity of the American trough increases correspondingly from its minimum in 1956 to its maximum in 1957 (figures not shown). Such negative correlation occurs also at other times. To present a qualitative estimation, we calculated the correlation coefficient of the variational tendency of the mean height of the two main troughs for any two years in the 30-year period from 1951 to 1980 (there are $c_{30}^{2} = 435$ sample points). The value of the correlation coefficient is -0.4 north of 45°N and 0.1 south of 45°N. The former is much higher than the 95% confidence level.

From the analysis of the relationship of the position and intensity of the polar vortex and the intensity variation of the two main troughs, we found that the negative correlation between the two main troughs is determined by the location of the polar vortex. The Asian trough intensifies and the American trough weakens when the polar vortex moves to the Eastern Hemisphere, and vice versa (figures not shown). To show this relation, we chose the 6 years (1956, 1966, 1967, 1969, 1973, and 1979) when the polar vortex stays in the Eastern Hemisphere and other 6 years (1953, 1957, 1962, 1972, 1974 and 1975) when the polar vortex remains in the Western Hemisphere for a composite analysis. Fig.1 shows the intensity (defined by the geopotential height on the trough line) variation with latitude of the two main troughs (Fig.1a) and the variation of geopotential height at 55°N with longitude (Fig.1b). We see that the Asian trough is weaker than the American trough when the polar vortex is located in the Western Hemisphere. From another point of view, the Asian trough becomes weaker when the polar vortex is in the Western Hemisphere than in the Eastern Hemisphere. The opposite conclusion holds for the American trough. Boger and Chen (1987) also obtained a negative correlation of

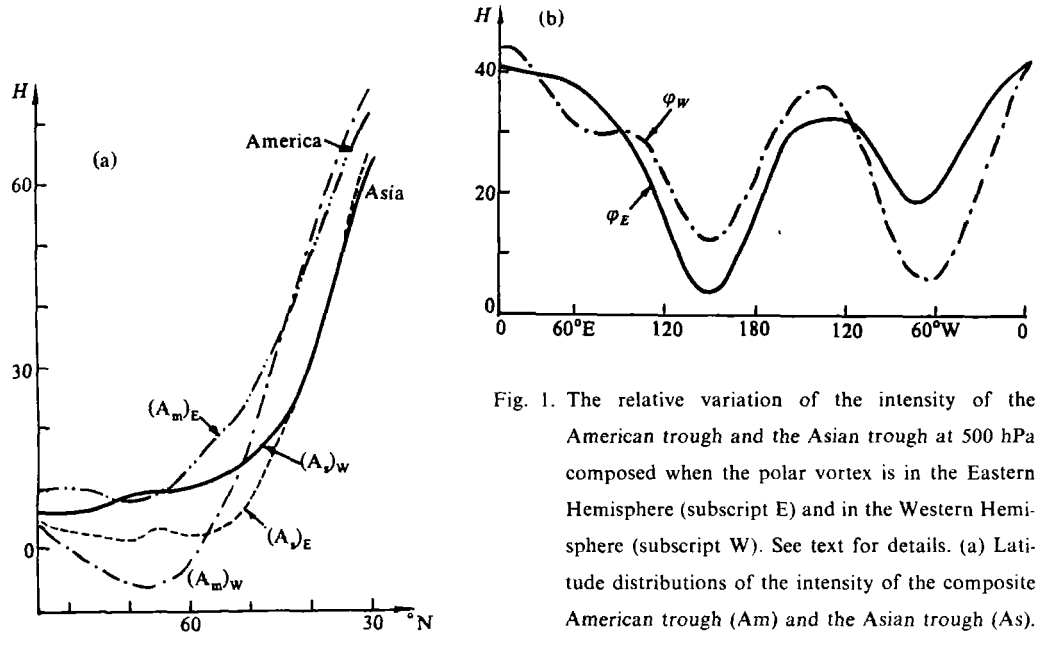

Fig. 1. The relative variation of the intensity of the American trough and the Asian trough at 500 hPa composed when the polar vortex is in the Eastern Hemisphere (subscript E) and in the Western Hemisphere (subscript W). See text for details. (a) Latitude distributions of the intensity of the composite American trough (Am) and the Asian trough (As). (b) Latitude variations of the composite geopotential height at 55°N (unit: dgpm).

the intensity of the two main troughs from their dishpan experiment while studying the influence of the Rocky Mountains and the Tibetan Plateau on the trough intensity in North America and East Asia (Figs.6 and 7 of their paper). Their experiment is for barotropic case. It seems that the negative correlation between the two main troughs is mainly related to the barotropic response of the orographic forcing of the general circulation.

2. *Contribution of Planetary–Wave to the American Trough and the Asian Trough*

Fig.2 shows the longitudinal distribution and mean–square variance of the two troughs at different latitudes. The Asian trough is generally wider and deeper than the American trough. The largest variation occurs at low latitudes and the smallest variation at middle latitudes for both troughs. The variance of the Asian trough reaches the minimum at 40°N , and that of the American trough at 50°N. Generally speaking, the variation of position of the American trough is larger than that of the Asian trough. Spectral analysis indicates that most of the transient mean square variance of the geopotential height on 500 hPa is related to the planetary waves (i. e., waves with wavenumbers 1, 2, and 3) (Fraedrich and Bottger, 1978). The amplitudes of planetary waves in a Fourier expansion of the geopotential height is far larger than the other waves. Therefore, the intensity and phase distributions of the planetary waves must have important impacts on the intensity of the two main troughs. Fig.3 presents the prevailing relationship among them using the 30–year data. The troughs of waves with wavenumber 1, 2 and 3 coincide on the east coast of Asia at middle latitudes (45°N and 30°N). The Asian trough is thus deepest at those latitudes (the minimum value is 476 dgpm). Since the ridge of wave 1 is located on the east coast of North America and where the troughs of wave 2 and wave 3 are located apart at 30°N, the North American trough is very weak at low latitudes. In high latitudes, the troughs of

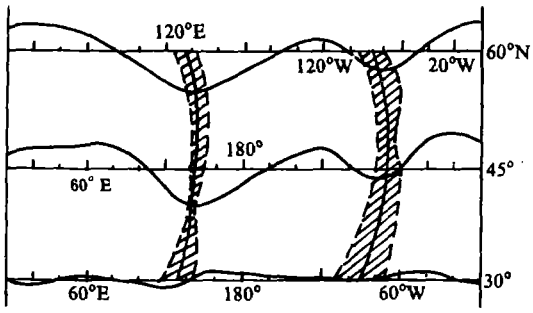

Fig. 2. Longitude distributions at different latitudes of the January mean geopotential height at 500 hPa from 1951 to 1980. The standard variance region is highlighted.

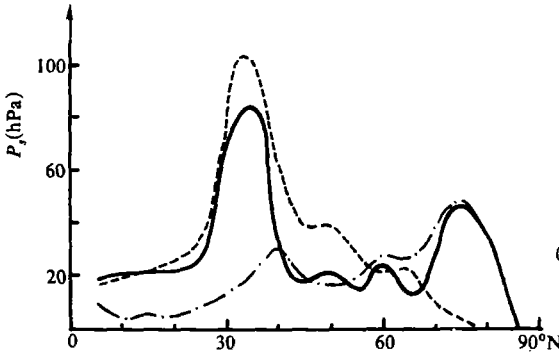

Fig. 4. Latitude variation of the wavenumber 1 amplitude of the standard surface pressure. Dashed curve: for the Eastern Hemisphere orography; dash–dotted curve: for the Western Hemisphere orography; and solid curve: for the Northern Hemisphere orography.

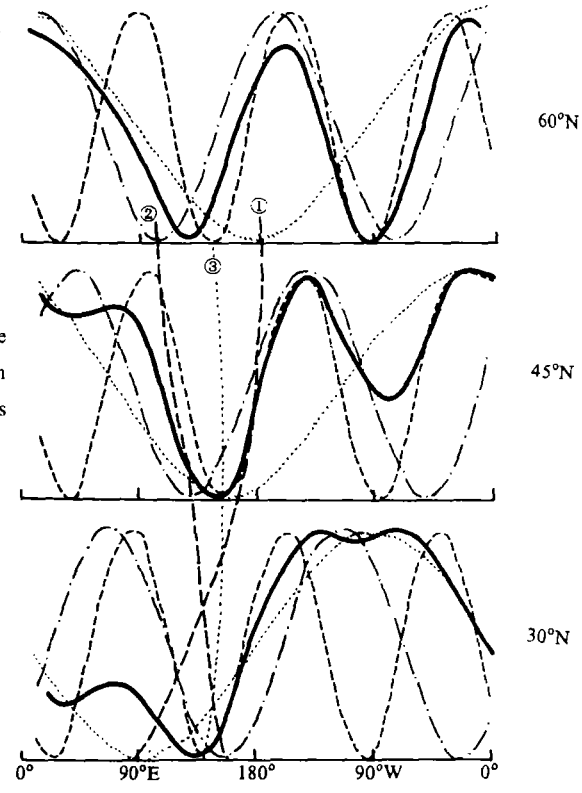

Fig. 3. The planetary wave components of the January mean geopotential height at 500 hPa from 1951 to 1980 at latitudes of 60°N (upper), 45°N (middle), and 30°N (lower). Dotted curve: wavenumber 1; Dash–dotted curve: wavenumber 2; Dashed curve: wavenumber 3; and heavy solid curve: composite of wavenumber 1 to 3. Notice that the amplitudes are all normalised. The vertical curves with encircled numbers indicate the latitude tilting of the corresponding troughs.

waves 2 and 3 almost coincide on the east coast of North America and since the amplitude of wavenumber 2 is most intensive in high latitudes (figures not shown), the composite American trough is then slightly stronger than the composite Asian trough (the minimum value for the former is 488 dgpm). Next we examine the orientation of troughs. Wave 1 goes from northeast to southeast with decreasing latitude, wave 3 behaves similarly and wave 2 goes from northwest to southeast. Since wave 2 is the strongest in high latitudes and waves 1 and 3 are stronger in the middle and low latitudes, the resulting climate mean trough goes , with decreasing latitudes.

from northwest to southeast in high latitudes and from northeast to southwest in middle and low latitudes.

One of the main reasons that the Asian trough is stronger than the American trough is that the trough of wavenumber 1 is located on the east coast of Asia. Such distribution of wave 1 seems to be related to the wavenumber 1 component of the orography since planetary waves in the upper troposphere are mainly related to orographic forcing. Fig.4 shows the latitude variations of the amplitude of orography in the Eastern and Western Hemispheres. The amplitude of the full orography in the Northern Hemisphere is also shown in the figure by the solid curve. We found that the wavenumber 1 component at middle and low latitudes in the Northern Hemisphere is mainly related to the orography in the Eastern Hemisphere. Therefore, the trough of wavenumber 1 at 500 hPa appears downstream of the Tibetan Plateau. In addition, Fig.4 also indicates that the intensities of the orographic wavenumber 1 in the Eastern and Western Hemispheres are comparable near 60°N, which reflects the wave 2 distribution of orography in the Northern Hemisphere. It is also consistent with the strong development of wave 2 in 500 hPa geopotential height at this latitude.

III. TELECONNECTION PATTERNS IN NORTH AMERICA AND EAST ASIA

When WG calculated the teleconnections from the monthly mean 500 hPa geopotential height field of the Northern Hemisphere, they found that there exist five "simultaneous teleconnection patterns". Many other researches also showed the existence of teleconnection patterns. We used the aforementioned 30-year data to study the relationship between orography and teleconnections. Altogether 3×4 points, which are downstream of the Rocky Mountains and the Tibetan Plateau and starting from (30°N, 90°W) and (30°N, 90°E) respectively, are selected as the key correlation points. They are spaced by $\Delta\lambda = 20^\circ$ and $\Delta\varphi = 15^\circ$. Upon using the correlation statistical method of WG, 24 teleconnection plots were then obtained. Analysis of these figures showed that, besides the 5 teleconnection patterns found by WG (figures not shown), there are other patterns which may be divided into three categories: the see-saw correlation pattern between high and low latitudes over the oceans, the North-America-Europe-Asia (NAEA) correlation pattern in middle and high latitudes, and the stationary wave chain downstream of the two main topographies.

1. *The See-Saw Correlation Pattern between High and Low Latitudes over the Oceans*

There exist negative correlations in geopotential height between high and low latitudes over the North Pacific and the North Atlantic Oceans, especially in the north and south sides of the jets, west of the two oceans (see Fig.5a). The western part of the West Pacific (WP) pattern, the West Atlantic (WA) pattern, and the East Atlantic (EA) pattern of WG belong to this type of teleconnection pattern. The existence of the see-saw correlation pattern might imply the interannual variation in the intensity of the jets since each jet is located in the middle of the corresponding see-saw pattern, downstream the two climate troughs. A strong jet corresponds to a strong north-south difference in the geopotential height, i.e., a negative (positive) height anomaly in the north (south), and vice versa. In addition, the polarities of the see-saws over the two oceans are opposite: there is a negative correlation between the correlation center in the

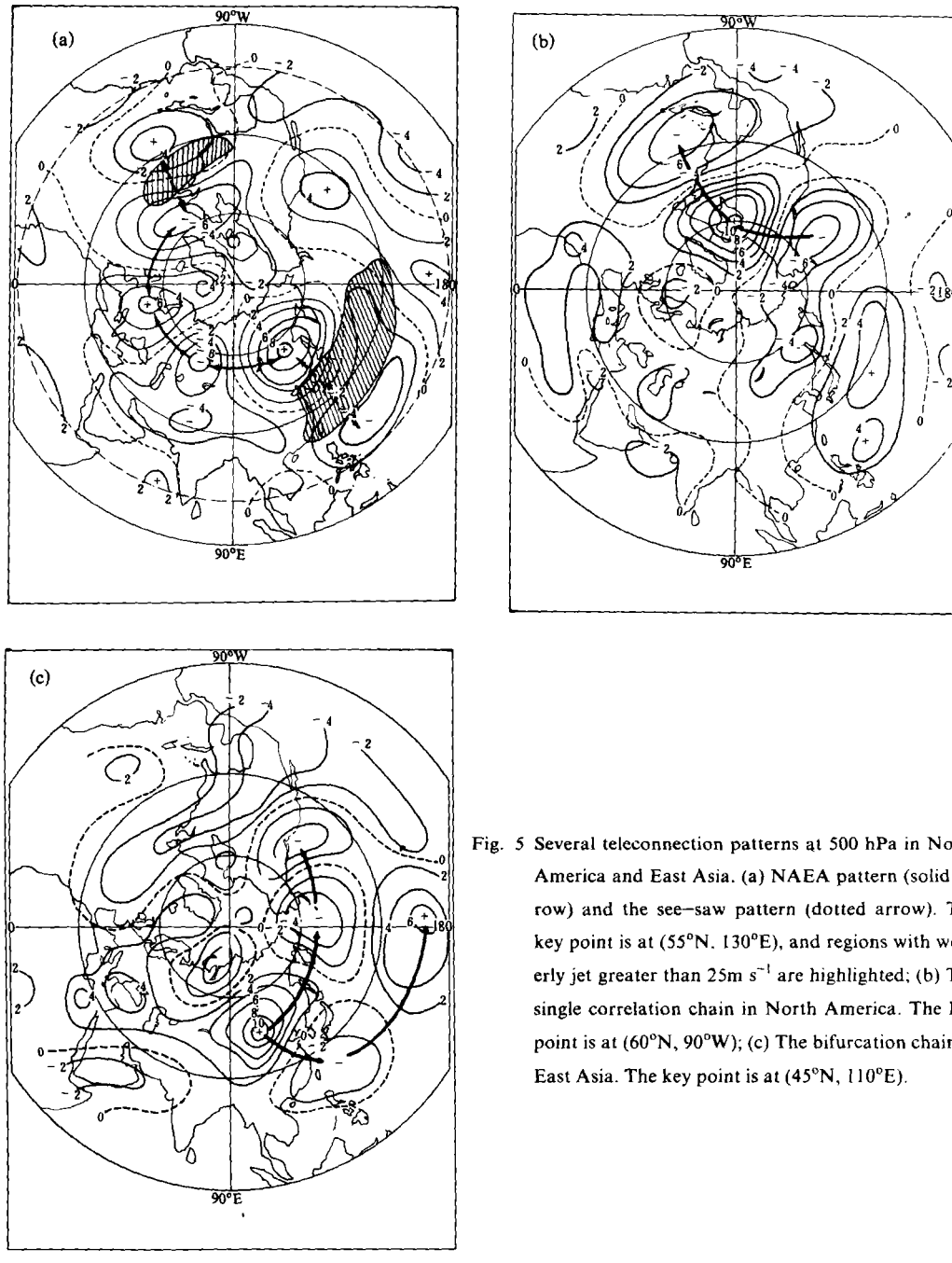

Fig. 5 Several teleconnection patterns at 500 hPa in North America and East Asia. (a) NAEA pattern (solid arrow) and the see–saw pattern (dotted arrow). The key point is at (55°N, 130°E), and regions with westerly jet greater than 25m s^{-1} are highlighted; (b) The single correlation chain in North America. The key point is at (60°N, 90°W); (c) The bifurcation chain in East Asia. The key point is at (45°N, 110°E).

east coast of Asia and that inNorth America in high latitudes. This is consistent with the previous discussion about the negative correlation of the intensity of the two main climate troughs. Therefore, this teleconnection pattern is probably related to the dynamic effect of the Rocky Mountains and the Tibetan Plateau as well as the orographically induced jet.

2. *The NAEA Correlation Pattern in Middle and High Latitudes*

Fig.5a shows the correlation pattern with the key point at (55°N, 130°E). There is a correlation chain in high latitudes from the Davis Strait, the northwestern Europe, to the east coast of Russia. This correlation chain is so obvious that it can be observed from all correlation maps with key points located north of 45°N. The eastern part includes the WG's EU pattern and the eastern part of EA pattern. The centre in its western part coincides with the northern centre of the WG's WA pattern. The correlation chain disappear or becomes the EA pattern if the latitude of the key point downstream of the orography is south of 45°N (figures not shown). Note that the opposite centre at both ends of this correlation chain is located on the two climate troughs. We indicated in the first part of Section II (see Fig.1) that the variation of the intensity of the two main troughs has a negative correlation north of 45°N. Thus the existence of this correlation chain in middle and high latitudes also reflects, to a large extent, the negative correlation of the two main troughs.

3. *Stationary Orographic Wave Chain*

Besides the aforementioned similar correlation patterns there exists different correlation pattern in North America and East Asia. In North America, negative correlations are located over the western coast of North America and western part of the Atlantic (see Fig.5b), when the key points are selected at (45°N, 90°W), (60°N, 90°W), (45°N, 70°W). They form a single correlation chain from middle and high latitudes to the equator. In East Asia, however, when the key points are chosen at (60°N, 90°E), (45°N, 90°E) and (45°N, 110°E), the correlation chain splits into south and north branches in middle latitudes, with one extending to the northeast and the other to the subtropics (see Fig.5c).

We should point out that the single correlation chain in North America is similar to the eastern part of the WG's Pacific North America (PNA) pattern. Although the statistics of WG did not indicate the bifurcation of the wave chain in East Asia, its existence can be proved from the following numerical experiments. Plumb (1985) calculated the 3–D EP fluxes using real data. The horizontal propagation of energy calculated by him is consistent with our bifurcation chain. We will show in the following section that the different wave chains in North America and East Asia are related to the horizontal propagation of stationary waves downstream of the two main mountains.

IV. THE HORIZONTAL PROPAGATION OF OROGRAPHIC STATIONARY WAVES

Rossby (1945) and Yeh (1949) studied the zonal wave propagation and energy dispersion problem, which was extended to spheric problems by Hoskins and Karoly (1981). They established the Rossby spherical wave dispersion theory. Held (1983) indicated that the structure of zonal flow has a strong influence on the behaviour of forcing waves. However, the distribution of zonal wind with longitude is in fact inhomogeneous and is related to the orographic effect (Bolin, 1950; Yeh, 1950) in the real atmosphere. In general, the jet in North America is located at higher latitudes. However, the jet in East Asia, which is stronger, is located at lower latitudes and normally has two branches with the southern branch being more stable. A nonlinear barotropic spherical primitive equation spectral model (Chen, personal communication) was

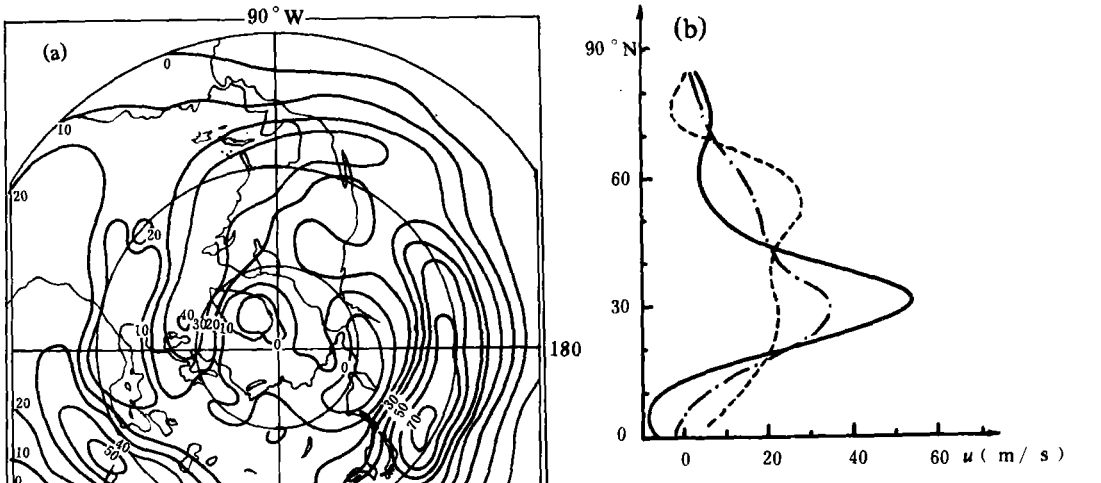

Fig. 6. Distributions of (a) the zonal wind u at 300 hPa in January 1983; and (b) the area mean value of u in region A (80°E— 140°W, solid curve), region B (120°W— 5°W, dashed curve), and in the Northern Hemisphere (dash– dotted curve). Units in m s^{-1}.

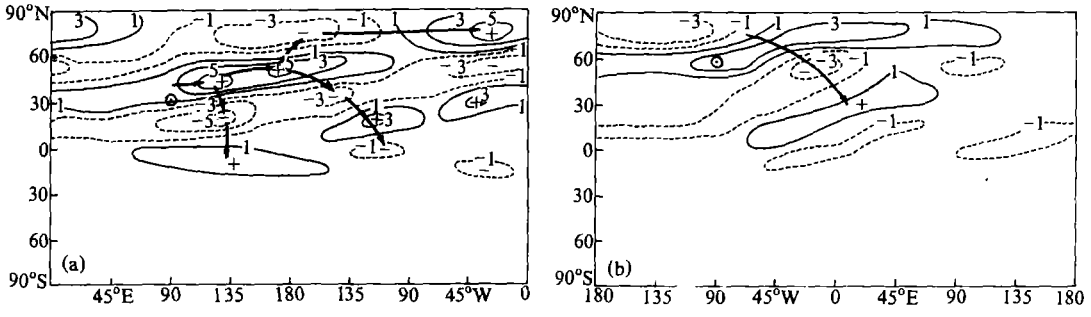

Fig. 7. Distributions of perturbation vorticity showing the quasi–stationary wave chains excited by stationary "orographic" perturbation source (circle) using a barotropic vorticity model (unit: 10^{-5} s^{-1}). (a) By using the u–distribution in region A with a perturbation source at 31°N; (b) By using the u–distribution in region B with a perturbation source at 57°N.

used to carry out numerical simulations in order to study the influence of orography and zonal wind distribution on teleconnection patterns. Numerical results will be analysed along with the theory of the Rossby spherical waves.

1. *Numerical Experiments*

Fig. 6a shows the distribution of January mean zonal wind on 300 hPa in 1983 (ECMWF data). We define area A as the region from 80°E—140°W, and area B from 120°W—5°W where the two main jets are located. The area–averaged zonal wind distribution is shown on

Fig. 6b.These zonal wind distributions are introduced into the vorticity equation as an Euler forcing, and the model was integrated 105 days to obtain a stable distribution of the jet in East Asia and North America. A single vorticity source was then added near the latitude of 31°N (57°N) once per day, and the model was integrated for 15 more days. The 15–day mean plots displayed in Fig.7 represent the response to these quasi–stationary perturbations. The perturbation in East Asia appears as a bifurcation when propagating eastward: one turns to the equator and the other to high latitudes. A second bifurcation appears at high latitudes. In North America, perturbation propagates consistently towards the equator. These two types of wave–chain distributions are very similar to the observation of the two correlation patterns downstream of the Rockies and Tibetan Plateau described in Section III.

According to the theory of Rossby spherical wave propagation, the wave amplitude satisfies the following equation:

$$\frac{\partial^2 \bar{\psi}}{\partial y^2} = \left(k^2 - B_m / U_m\right)\bar{\psi}, \tag{1}$$

where k is the zonal wavenumber and a Mecator coordinate system (projection) was used. The critical wavenumber K_s of propagating waves is

$$K_s \equiv (B_m / U_m)^{1/2} = \left\{\frac{1}{U}\left[\frac{2\omega}{a}\cos^3\varphi - \cos^2\varphi\frac{\partial}{\partial\varphi}\frac{1}{\cos\varphi}\frac{\partial}{\partial\varphi}(u\cos\varphi)\right]\right\}^{1/2} \tag{2}$$

From Eq.(1) we know that waves with wavenumber $k < K_s$ can propagate southward or northward, while waves with $k > K_s$ are decaying waves or "trapped" waves. Fig.8 shows the distributions of critical wavenumbers as a function of latitude based on the real data presented in Fig. 6b. There is a wide "trap" near the jet latitudes (φ_j: 30—35°N) in East Asia. Only waves with wavenumbers smaller than 3 can propagate toward high latitudes through this latitude band. Waves with wavenumber greater than 3 can not propagate through this "trapped" band and will turn southward at some turning latitude φ_T. Therefore, the dispersion occurs at the jet region, and wave chain appears as a "bifurcation". Downstream of the Rocky Mountains, critical wavenumber decreases monotonously with increasing latitudes and becomes very small near 60°N. Large–scale waves excited by the Rocky Mountains all turn to propagate southward not far away from the source region. These analyses are also in consistence with the results of numerical experiment presented in Fig.7, and can be used to explain the difference between the teleconnection pattern in North America and East Asia.

2. *Impact of the Westerly on Wave Propagation and Bifurcation*

The north–south wavenumber is equal to zero at the turning latitude φ_T, since wave only propagates eastward there, i.e.,

$$k = K_s, \qquad \text{if} \qquad \varphi = \varphi_T. \tag{3}$$

Assuming $\beta \gg \partial\bar{\xi} / (a\partial\varphi)$, from Eqs.(2) and (3) we have the following approximation

$$\frac{2\Omega\cos^3\varphi}{ak^2 u} - 1 = 0, \qquad \text{if} \qquad \varphi = \varphi_T, \tag{4}$$

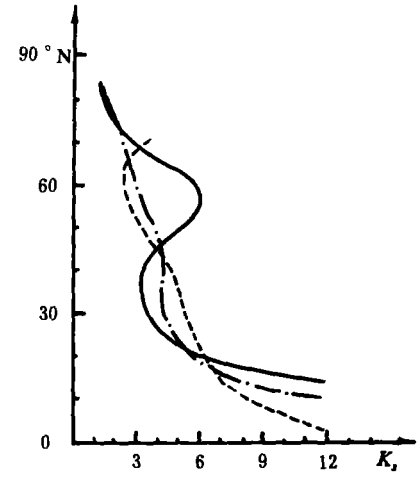

Fig. 8. Variations with latitude of the horizontal critical wavenumber in correspondence to the zonal wind data shown in Fig.6b. Solid, dashed, and dash–dotted curves denote the distributions in region A, region B and in the Northern Hemisphere, respectively.

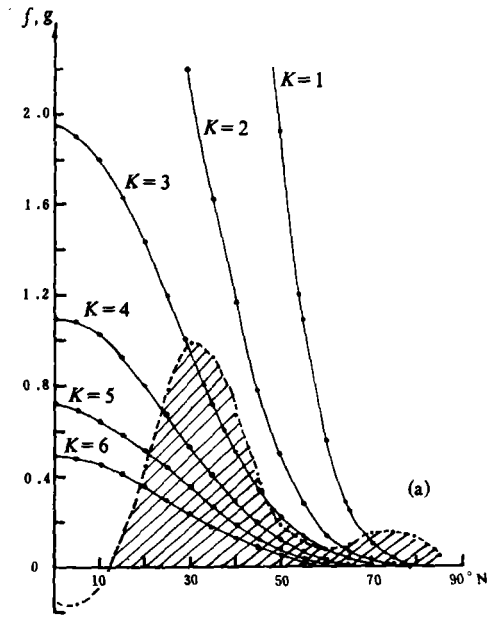

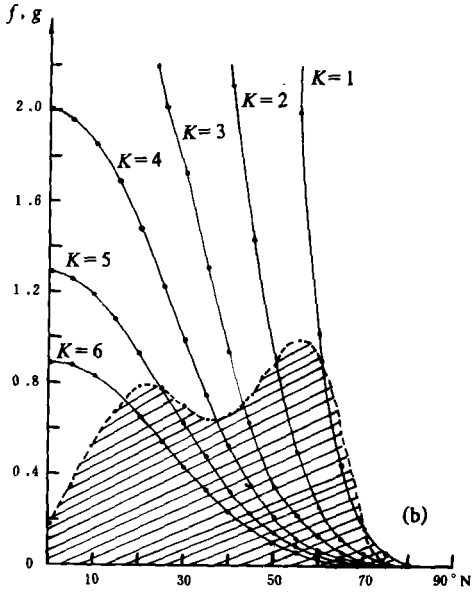

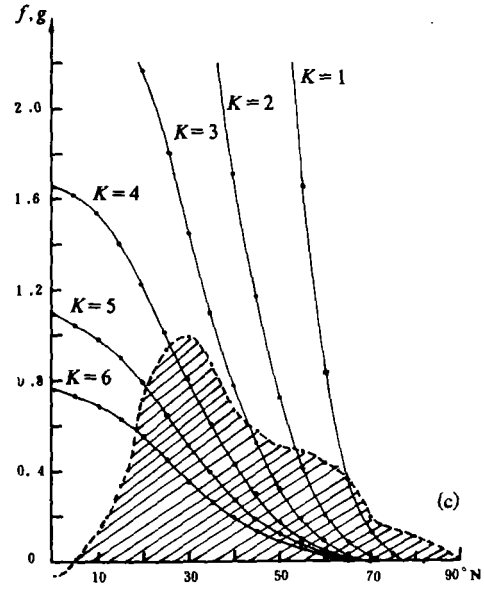

Fig. 9. Latitude distributions of the function $f(\varphi,k,U)$ (solid curve) and $g(\varphi)$ (dashed curve). (a) In Region A (80°E —140°W), (b) in Region B (120°W—5°W), and (c) in the Northern Hemisphere.

which has a higher accuracy in weakly shear flow and lower accuracy in strong shear flow and at high latitudes. However, the latter does not affect our following qualitative discussions.

Introducing a scalar function of latitude $g(\varphi)$ so that

$$u = Ug(\varphi), \tag{5}$$

where U represents the maximum zonal wind, and defining

$$f(\varphi,k,U) = F\cos^3\varphi, \tag{6}$$

where $F = 2\Omega / (ak^2 U)$, we obtain from (4) an equation that wavenumber k should satisfy at the turning latitude φ_T:

$$f(\varphi,k,U) = g(\varphi), \qquad \varphi = \varphi_T. \tag{7}$$

This equation can be solved schematically and the turning latitude φ_T can be obtained from the intersecting points of the two curves f and g. From Eqs.(2), (5) and (6) we have

$$f(\varphi,k,U) / g(\varphi) = (K_s / k)^2. \tag{8}$$

Therefore, the condition $g(\varphi) > f(\varphi,k,U)$ defines the "trapped" region for wave propagation. At the jet latitude φ_J, $g(\varphi_J) = 1$, the dispersion condition becomes

$$f(\varphi_J,k) < 1, \qquad k > K_s \tag{9}$$

$$f(\varphi_J,k) > 1. \qquad k < K_s \tag{10}$$

Eq.(9) is a necessary condition for the existence of a turning latitude of wavenumber k. In other words, a turning wave is a "trapped" wave at the jet axis.

Fig.9 shows the distribution of f and g in North America and East Asia calculated from Eqs.(5) and (6) by using the zonal wind data shown in Fig.6b. The highlighted region represents the "trapped" area. From Fig.9a we see that in East Asia, planetary waves with wavenumbers 1 and 2 can propagate northward through the jet band (φ_J) and waves with wavenumber greater than 2 will be "trapped" and turned towards south. Wave propagation there thus appears as a "bifurcation". In North America (Fig.9b), however, all waves, except wavenumber 1, satisfy (3). They are "trapped" in the jet region (near 55°N) and propagate southward. The wavenumber 1 propagating northward satisfies (3) for a short while but turns also towards south due to the fact that at higher latitude the critical wavenumber K_s approaches zero rapidly. Therefore, perturbations excited by the orography in high latitudes propagate southeastward consistently. This explains the simulated results displayed in Fig.7. When the zonal mean flow in the Northern Hemisphere is used, wave propagation still appears as a "bifurcation" (Fig.9c). However, the wave with wavenumber 3 also can propagate to the north, which is different from the result obtained by using the area mean zonal flow in East Asia (Fig.9a) and is consistent with the results of Grose and Hoskins (1979). In fact, for a given location of the jet φ_J, according to Eqs.(6) and (9), the turning condition for wavenumber k is

$$U > \frac{2\Omega}{ak^2}\cos^3\varphi_J. \tag{11}$$

When $\varphi_J \approx 30°$N, the turning condition for wavenumbers 3 and 4 is that the intensity of the jet (U) should be greater than 50 and 28 m s^{-1}, respectively. Since U is equal to 58 and 35 m s^{-1}

in East Asia and in the Northern Hemisphere, the wave with wavenumber 3 is a turning wave in East Asia, but becomes a propagating wave under the Northern Hemisphere zonal mean flow.

Analysis in this section indicates that whether bifurcation of a wave chain occurs depends tightly on the latitude location of the jet. The intensity of a jet can influence the wavenumbers of propagating waves, but it has less impact on its "bifurcation". The jet in East Asia is located at low latitudes, which causes a bifurcation of propagating wave and "trapped" wave near the jet axis. On the other hand, the jet in North America is located at high latitudes and waves propagate consistently towards the equator. Such difference of the stationary wave propagation in the two regions can be used to explain the difference in teleconnection patterns in Norht America and East Asia shown in Fig.5.

V. CONCLUSIONS

In high latitudes the troughs in North America and East Asia possess comparable intensity and tilt from northwest to southeast. In middle and low latitudes the Asian trough is stronger than the American trough and both troughs tilt from northeast to southwest. There exists a strong negative correlation in the intensity and variation of the two troughs, which are related to the location of polar vortex. The Asian trough is stronger than the American trough when the polar vortex is in the Eastern Hemisphere and vice versa.

The analysis of the teleconnection patterns of the January mean geopotential height at 500 hPa indicates that there exist similar see–saw and NAEA teleconnection patterns in East Asia and North America. The see–saw pattern over the two oceans is related to the interannual variation of the jet intensity. The NAEA pattern reflects the negative correlation between the variation of the two troughs in East Asia and North America. The aforementioned similar distribution of the teleconnection pattern in East Asia and North America is in fact the reflection of common dynamic effects of the two main mountain blocks in the Northern Hemisphere.

There also exist different teleconnection patterns in East Asia and North America. A single wave chain exists in North America while a bifurcation wave chain occurs in East Asia with one branch propagating towards northeast and the other towards southeast. Numerical experiment and theoretical analysis indicate that this difference in correlation patterns is related to the difference in the propagation of the orographically induced stationary waves in these regions. In North America the jet is at high latitudes, critical wavenumber increases with decreasing latitudes and waves propagate consistently towards the south. In East Asia, the jet is located in the subtropics, critical wavenumber has a "trapped" region. Only waves with low wavenumbers can propagate northward through the "trapped" region; waves with high wavenumbers are "trapped" waves propagating southward. It is this dispersive phenomenon of waves which causes the wave chain to appear "bifurcated".

It is therefore concluded that the structure and variation of the trough and ridge at 500 hPa, the distribution of teleconnection patterns, and the propagation characteristics of quasi–stationary waves are all correlated to each other. They are closely related to the dynamic effects of the two main mountain blocks in the Northern Hemisphere.

REFERENCES

Blackmon, M. L., Wallace, J. M., Lau N.–C. and Muller, S. L. (1977), An observational study of the Northern Hemisphere winter circulation, *J. Atmos. Sci.*, **34**: 1040—1053.

Boger, Don. and Chen Rui-Rong (1987), Laboratory simulation of mechanical effects of mountains on general circulation of Northern Hemisphere: Uniform shear background flow, *J. Atmos. Sci.*, **44:** 3552—3573.

Bolin, B.(1950), On the influence of the earth's orography on westerlies, *Tellus*, **2:** 184—195.

Charney, J. G. and Eliassen, A. (1949), A numerical method for predicting the perturbations of the middle latitude westerlies, *Tellus*, **1:** 38—54.

Fraedrich, K. and Bottger, H. (1978), A wavenumber-frequency analysis of the 500 mb geopotential at 50°N, *J. Atmos. Sci.*, **35:** 745—750.

Gambo, K. (1956), The orographic effect upon the jet stream in the westerlies, *J. Meteor. Soc. Japan*, **34:** 24—28.

Grose, W. L. and Hoskins, B. J. (1979), On the influence of orography on the large scale atmospheric flow, *J. Atoms. Soc. Sci.*, **36:** 223—234.

Held, I. M. (1983), Stationary and quasi-stationary eddies in the extratropical troposphere: theory, *Large-Scale Dynamical Processes in the Atmosphere*, B. Hoskins and R. Pearce, Eds, Academic Press, pp.127—158.

Hoskins, B. J. and Kalory, D. J. (1981), The steady linear response of a spherical atmosphere to thermal and orographic forcing, *J. Atmos. Sci.*, **38:** 1179—1196.

Hoskins, B. J. , Simons, A. and Andrews, D. G. (1977), Energy dispersion in a barotropic atmosphere, *Quart, J. Roy. Meteor. Soc.*, **103:** 553—556.

Jacqmin, D. and Lindzen, R. S. (1985), The causation and sensitivity of the north winter planetary waves, *J. Atmos. Sci.*, **42:** 724—745.

Kasahara, A. (1966), The dynamical influence of orography on the large-scale motion of the atmosphere, *J. Atmos. Sci.*, **23:**259—271.

Kasahara, A., Sasamori, T. and Washington, W. N.(1973), Simulation experiments with a 12-layer stratospheric global circulation-model, I. Dynamical effect of the earth's orography and thermal influence of continentality,*J. Atmos. Sci.*,**30:** 1229—1251.

Lau,N.-C. (1978), On the three-dimensional structure of the observed transient eddy statistics of the Northern Hemisphere wintertime circulation, *J. Atmos. Sci.*, **35:** 1019—1023.

Lau, N.-C. (1979), The observed structure of tropospheric stationary wave and the local balance of vorticity and heat, *J. Atmos. Sci.*, **36:** 996—1016.

Murakami, T. (1956), The orographic effects in the three-level model of the *s*-coordinate, *papers in meteorology and geophysics*, Tokyo Meteorological Research Institute, Japan, **14:** 144—150.

Nigam, S. (1983), On the structure and forcing of tropospheric stationary waves, Ph. D. thesis, Princeton University.

Plumb, R. A. (1985), On the three-dimensional propagation of stationary waves, *J. Atmos. Sci.*, **42:** 217—229.

Rossby, C.-G. (1945), On the propagation of frequencies and energy in certain types of oceanic and atmospheric waves, *J. Meteor.*, **2:** 187—203.

Wallace, J. M. and Gutzler, D. S. (1981), The teleconnections in the geopotential heigh field during the Northern Hemisphere winter, *Mon. Wea. Rev.*, **109:** 784—812.

Yeh, T. C. (1949), On energy dispersion in the atmosphere, *J. Meteor.* , **6:** 1—16.

Yeh, T. C. (1950), The circulation of the high troposphere over China in the winter of 1945—1946, *Tellus*, **2:** 173—183.